

Assessment of Computational Cell Model Benefits for Optimization of Microfluidic Devices

Alžbeta Bohiniková¹ ^a, Inês Maia^{2,3} ^b, Monika Smiešková¹ ^c, Alžbeta Bugáňová¹ ^d,
Ana S. Moita² ^e, Ivan Cimrák¹ ^f and Rui A. Lima^{3,4} ^g

¹Cell-in-Fluid - Biomedical Modeling and Computation Group, University of Zilina, Slovakia

²IN+ Center for Innovation, Technology and Policy Research, Instituto Superior Técnico, Universidade de Lisboa, Av. Rovisco Pais, 1049-001 Lisboa, Portugal

³Metrics, Mechanical Engineering Department, University of Minho, Campus de Azurém, 4800-058 Guimarães, Portugal

⁴CEFT, Faculdade de Engenharia da Universidade do Porto (FEUP), R. Dr. Roberto Frias, 4200-465 Porto, Portugal

Keywords: Computational Cell Model, Microfluidic Devices, Cell Deformation.

Abstract: This article describes the overview of the steps required to derive and validate a new model on cell behaviour in microfluidic devices, from the experimental approach to the computational model. The paper identifies the challenges of the biological side of the experiments and shows where computational power can be useful. It also emphasizes the necessity for the collaboration between the experimental and computational research groups. Computations can offer great insights into the mechanics of cells, however, interesting applications mainly arise from combining numerics with experiments. Well calibrated and verified model can be used to improve the performance of a given microfluidic device by testing various geometries and thus lowering the number of devices that need to be produced. Choosing several designs of microfluidic devices one tries to demonstrate the wide range of possible uses of the microfluidic technology and how the computations can enrich them.

1 INTRODUCTION

There is a rising necessity for interdisciplinary cooperation in solving problems in microfluidics. Microfluidic devices have a broad spectrum of use, ranging from devices for sorting cells based on their mechanical properties to devices designed to detect specific cells or even to study mechanical properties of individual cells (Sajeesh and Sen, 2014). Especially, the use for clinical purposes can have a great influence on the early diagnosis of metastatic cancer and thus can help patients to get personalized treatment (Zhang and Nagrath, 2013).


There is a variety of microfluidic devices based


on their intended use. When interested in measuring the biophysical properties of single cells, most common are devices with narrow channels and obstacles, where transition times and deformation coefficients can be measured.


A microfluidic device consisting of a straight channel with constriction ($150 \times 10 \times 10 \mu\text{m}$) was used in (Hou et al., 2009). The study aimed to determine differences between cancer line cells MCF-10A (benign breast epithelial cell) and MCF-7 (non-metastatic tumor breast cell). This work was the inspiration behind the production of the microfluidic channels described in Section 3.3.


Other types of devices, such as ones used in (Lima et al., 2008) and (Pinho et al., 2013), focused on global properties of the dense blood suspensions. There is large number of microfluidic devices being developed for in vitro cancer diagnosis (Chen et al., 2012).


The need to improve these devices is ever increasing (Shields IV et al., 2015). This process is costly and time consuming. Computational models of cells


^a  <https://orcid.org/0000-0001-8058-7929>


^b  <https://orcid.org/0000-0001-7986-8934>

^c  <https://orcid.org/0000-0002-3633-1798>

^d  <https://orcid.org/0000-0001-6772-2970>

^e  <https://orcid.org/0000-0001-9801-7617>

^f  <https://orcid.org/0000-0002-0389-7891>

^g  <https://orcid.org/0000-0003-3428-637X>

and their flow in microfluidic devices can help improve their design and save time by lowering the amount of necessary lab experiments.

To help with this process, we started a collaboration between Cell-in-fluid Biomedical Modelling & Computations Group (CifBMCG), the Laboratory of Interfacial plus Microscale Phenomena from IN+, Centre for Innovation, Technology and Policy Research in Instituto Superior Técnico, Universidade de Lisboa and Metrics research center, from University of Minho. Here we present the main goals of the research project behind this collaboration and some initial results gathered.

1.1 ESPResSo and PyOIF

Simulation model used for this work is being developed by our research group at the University of Zilina. All the computations are run on ESPResSo (Weik et al., 2019) software with an open source license. We developed the python module PyOIF¹ that allows modelling of blood as a fluid with immersed elastic objects, which represent blood cells. More information can be found in (Cimrak et al., 2014).

There are two main parts of the model, namely the model of the fluid and the model of the elastic object, that are coupled by dissipative forces. More details can be found in (Busik and Cimrak, 2017).

The fluid is modelled using the lattice-Boltzmann method. The space, through which the fluid moves is represented by a lattice of discrete points. With this method, the points are fixed throughout the whole simulation. During the simulation, fictitious fluid particles move and encounter other particles, which transfer information about their velocity and direction. Information about the number and speed of the particles passing through each of the fixed lattices is stored. In-depth description of this method can be found in (Cimrak and Jancigova, 2018).

1.2 Computational Model of Elastic Cell

The model of elastic cells is represented by an approximation of the cell membrane surface. Five elastic moduli are responsible for the elastic behaviour of the cell. Next section provides a brief overview of these parameters. More details are presented in (Cimrak and Jancigova, 2018).

The stretching modulus is responsible for the rigidity of the cell. Once the cell membrane is stretched, this modulus reacts and develops resistance against the stretching force to achieve the original relaxed state of the cell. The edges of the triangles can

be thought of as springs trying to stay in their original relaxed length.

The bending parameter aims to maintain the shape of the object by preservation of the angles. The triangle mesh has a prescribed relaxed state and this modulus maintains the angles between neighboring triangles.

Local area conservation parameter manages preservation of individual triangle area. When the cell deforms by pressing forces and the areas of the triangles change, this parameter is responsible for applying forces to achieve the original area.

The three parameters described above are related to local regulation of the cell shape. The following two parameters will guarantee the conservation of global properties such as the global cell surface and the cell volume.

Global area conservation preserves constant surface of the whole object. If the surface of the cell is larger than desired, this parameter acts to decrease this surface. On the opposite, if it is smaller, this parameter increases it. There is a control system for the surface of the cell. When the relative changes are too large (larger than 3%), the simulation stops with a warning.

The global volume conservation parameter is similar to the global area conservation parameter, but instead of surface, it is responsible for global volume. It maintains constant volume of the cell during the simulation. Similarly as for the global area conservation parameter, there is control system which stops the simulation with a warning in case the cell volume becomes larger than 3%.

The model of RBCs was calibrated using the stretching experiment (Dao et al., 2003), where silica beads were attached to the cell and afterwards the cell was stretched with different forces and the change in cells radial and axial size was measured. The model was also validated with experimental data of RBC deforming in a flow (Kovalcikova, 2019).

When setting up simulations of real biological experiments, the most important is to set the parameters as closely as possible to the experimental environment. Apart from channel geometry and visco-elastic properties of the fluid, which are set based on the experiments, and elastic parameters of the cell that are set based on the calibration, one must also consider the flow of the fluid in the channel. This information is quite challenging to obtain from the biological experiments, especially in narrow channels, such as the ones used in 3.3. This is because at low volumetric rate, the suspension might not even pass through and at higher rates the flow may become too fast to be captured for instance by a high-speed camera (it

¹<http://cellinfluid.fri.uniza.sk/resources-espresso/>

can be out of the range of camera capture capacities). Running simulation with the volumetric flow rate of was $2.5\mu\text{L}/\text{s}$ resulted in higher velocities than those measured from the biological experiment. Thus we established the simulation flow by comparing the cell velocities.

2 BIOLOGICAL EXPERIMENTS

The biological experiments for this work were carried out and recorded at Metrics research center in University of Minho, in cooperation with the Laboratory of Interfacial plus Microscale Phenomena from IN+, in University of Lisbon. Different types of microfluidic channels were tested to present various typical cases addressed in microfluidic technology. The details on the properties and origins of cells used for these experiments are outlined in Section 2.2.

2.1 Experimental Setup

The flow of the working fluid was analyzed with a system constituted by an inverted microscope (IX71, Olympus) and a high-speed camera (FASTCAM SA3, Photron). The microfluidic devices were placed on the stage of the inverted microscope and a syringe pump (CetoniNEMESYS Syringe Pump) was used to produce a constant flow rate.

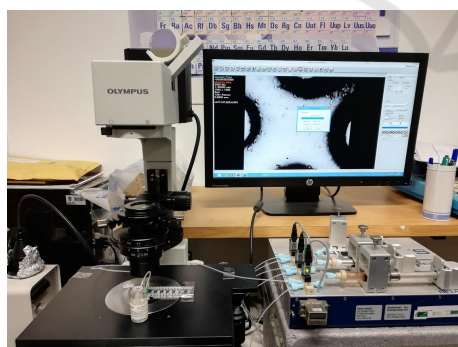


Figure 1: Experimental setup.

2.2 Biological Material

The working fluid used in the experiments was a suspension of human red blood cells (RBCs) in dextran 40 (Dx40) with a hematocrit (Hedct) of 0.2%. In brief, blood from healthy individuals was obtained from Instituto Português do Sangue e da Transplantação (IPST). The RBCs were separated from bulk blood by centrifugation (1500 rpm for 15

min) and then the plasma was removed by aspiration. The RBCs were then washed with a physiological saline solution and the process was repeated two more times. Lastly, the RBCs were diluted with Dx40 to make up the required concentration.

2.3 Microfluidic Devices

In this study, four different types of channels are addressed. Spiral sorter chip and Pillar chip were obtained from microfluidic ChipShop. The other two chips were produced in Metrics research centre in the University of Minho. The production process of the latter two is described in Section 2.3.1. For each type of microchannel, the potential use and how can the computational model be used are outlined.

2.3.1 Production of Microfluidic Devices

The microchannels used in this work were produced by a soft lithographic technique. Firstly, to fabricate the master moulds, the geometries were drawn in AutoCAD to produce a high-resolution photomask. The mould was then fabricated on a silicon wafer with an ultrathick photoresist (SU-8 50; Kayaku MicroChem, Japan). The polydimethylsiloxane (PDMS) prepolymer was prepared by mixing a commercial prepolymer and a curing agent (Silpot 184; Dow Corning, USA) at a 10:1 weight ratio. The mixture was degassed under vacuum and the PDMS was poured into the SU-8 photo-resist master mould and cured in an oven for about 2 h at 70°C . After both master and PDMS were cooled to room temperature, the PDMS was peeled from the master. The input and output ports are made using micro-pipette tips. Lastly, the PDMS was washed with ethanol and spin-coated over a clean glass slide. The microchannels were manufactured considering three different heights, namely $31\mu\text{m}$, $25\mu\text{m}$ and $12\mu\text{m}$. The geometry of the microchannel with the tallest height is presented in Figure 5.

3 MICROFLUIDIC DEVICES DESIGNS AND POTENTIAL OF COMPUTATIONAL CELL MODEL

3.1 Spiral Sorter

One of the short term goals of the CifBMCG is to design and construct geometry for special spiral channels utilizing inertial effects for cell sorting. Such a

device can be used for ultra-fast cancer cells filtering without labelling from blood (Warkiani et al., 2014).

The technique utilizes the natural Dean vortex flows present in the continual flow inside curvilinear microchannels along with inertial lifting forces that concentrate larger cancer cells against the inner wall. By using spirals and circular cross-section, unlike the traditional rectangular cross-section, the position of the Dean's vortex core can be altered to achieve separation. Smaller hematologic components are trapped in Dean's vortices slanted toward the outer walls of the duct and finally removed at the outer outlet, while larger cancer cells accumulate at the inner wall of the channel and collect from the inner outlet.

The plan is to start with a single spiral micro-channel with one input and two outputs. This arrangement could successfully isolate two types of cells with different mechanical properties. Simulations can be used to suggest how to position the outputs in order to achieve better purity in the filtering process. Running biological experiments with healthy and sick RBCs pushed through the different channels in the microfluidic device in Figure 2 can be used to validate the model in this novel geometry. Afterwards, the simulations can be used to design improved devices which then can be produced and tested. Next step could be to use this device to sort cancer cells from the blood.

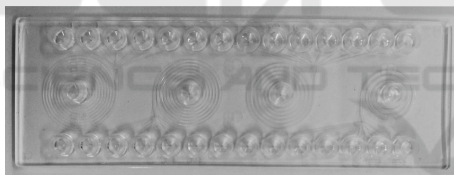


Figure 2: Spiral sorter chip.

3.2 Pillar Channels

There are many biological studies focusing on the flows in different geometries that can be characterized by the common property of having arrays of periodic pillars.

Cell-in-fluid research group already carried out simulation studies of channels inspired by such biological experiments (Nagrath et al., 2007), (Huang et al., 2004), (Inglis et al., 2006), (Gleghorn et al., 2010). However, the simulation results could only be compared with data collected from the literature, which did not include all the required information to fully validate the numerical model.

Our previous studies concerned the trajectories and rotation of the cells (Bachratý et al., 2017), (Slavík et al., 2017) and (Kovalčíková et al., 2018). Since computational power is somewhat limited, only

part of the microfluidic devices was simulated, with periodic borders. This means that one can only obtain local information on the behaviour of the cells and then extrapolate conclusions for the overall behaviour. This was studied in (Chovanec et al., 2019).

In order to further develop our research in this area a microfluidic chip with several channels with different pillar geometries was now chosen (see Figure 3). The flow in one of the channels of this microfluidic chip was recorded using the high-speed camera (as aforementioned), from which data can be obtained in post-processing processes, according to the following three steps process.

- Video Processing - Currently, there are various software packages available that can be used for tracking cell trajectories and obtaining information about the cell deformations, such as ImageJ. However, using these is either a manual or semi-manual process. There are also limitations concerning the shape of trajectories, as ImageJ can only track straight trajectories, for example. One of the goals is to automatize this step. First steps towards achieving this goal have already been taken, see (Kajánek and Cimrák, 2019).
- Simulations - We will simulate part of the device, that can be seen on the recordings from the experiment, see Figure 5. Comparing the cell trajectories from simulations with the trajectories of actual cells will serve as validation of the model. Afterwards, it is possible to perform a computational study with different geometries from the chip and then carrying out reverse comparison where we should confirm that the cell behaviour predicted by our model is similar to that of the real cells. With this double verification, we can further study other possible geometries and further optimize the model, for example, to achieve higher collision rates with the pillars or introduce other types of cells.
- Statistical Analysis - Using machine learning techniques, specifically convolutional neural networks, we aim to predict cell behaviour within large microfluidic devices. Simulations of whole microfluidic devices require excess computational power, which is limited. To overcome this, we plan to use both the information obtained from videos of biological experiments and data from simulations in order to compare the results of our techniques, building on the work started in (Chovanec et al., 2019).

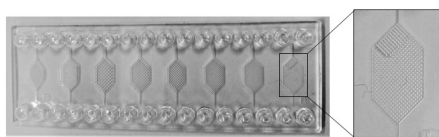


Figure 3: Pillar chip.

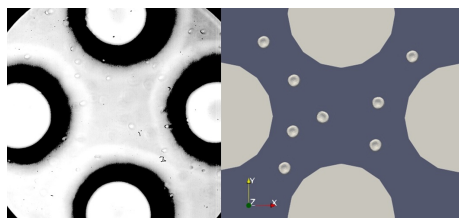


Figure 4: Capture from the video recording of the experiment on the left side. Example of cell seeding in simulation with the pillar geometry on the right.

3.3 Channels with Constriction

With these types of channels, the objective is to study the deformation of individual cells. As a starting point, we looked at the deformation of a healthy RBC. Further experiments will be carried out, once there are other types of cells available. Particular emphasis is expected to be given to studies on the deformation of cells with a nucleus. This could be then used to study the flow of rare cells, such as the circulating tumour cells, in the microfluidic devices and optimize their geometry to achieve the desired properties.

Production of these devices is described in Section 2.3.1. The Metrics research centre in the University of Minho already produced similar geometries in (Boas et al., 2018). The objective now is to go smaller and achieve the flow of cells in one layer which should allow for a better focus of the video recordings.

Several videos were captured, however, there were some challenges with the volumetric flow rate, as mentioned in Section 2.1. We analyzed one of these videos where the volumetric flow rate on the pump was set to $2.5 \mu\text{L}/\text{s}$. Once the simulations finish we plan to compare the numerical and experimental results by looking at the time required for the cell to pass through the channel and at the deformation index (DI). Figures 7 and 8 depict the partial results gathered so far.

Furthermore, several sections were selected from the channel and will be used to qualitatively compare the shape of the cell deformation obtained from the experiments and the numerical results.

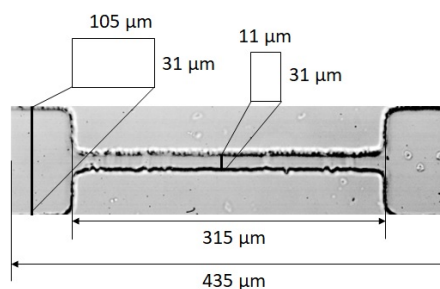


Figure 5: Dimensions of the channel with constriction.

3.3.1 Data Processing

As aforementioned the quantitative data was extracted from video recordings of the experiments, using ImageJ (Schneider et al., 2012). For each cell, deformation index, velocity, constriction time and average velocity in constriction were measured. To obtain the DI a boxing rectangle was created for each frame. DI was computed as $|x - y| / (x + y)$, where x is the width and y is the length of the rectangle. There are other options to determine the DI, but this was chosen due to simplicity in terms of how easy it is to compare the experimental data with the numerical results in this case.

3.3.2 Comparison between Numerical and Experimental Results

Due to the difficulties with the reliability of the volumetric flow rate, as already discussed in Section 2.1, the flow velocity was evaluated instead and used to set up the fluid flow in the simulation. The parameter of fluid force density was set to 0.0003.

The position of the biological cells was analyzed when entering the narrow part of the channel. From 16 cells detected in the video, 12 passed through the whole length. 5 cells entered in the middle and 6 from the top. Upon entering, most of the cells were rotated vertically in the flow direction, see Figure 6.

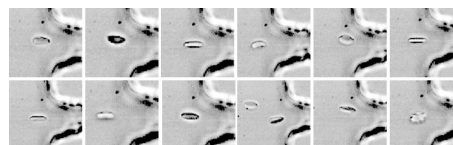


Figure 6: All 12 cells at the entrance of the constriction.

Figure 7 depicts the difference between the cell deformation when the cell is starting centred (the grey cell) in the middle and when the cell is moved $5 \mu\text{m}$ to the left (the red cell). The simulation is still running and our results go up to one-third of the constriction. So we show the difference at the entrance

(Figure 7 A), then $20\ \mu\text{m}$ (Figure 7 B) into the constriction and then in the middle (Figure 7 C). The difference in the DI changes, depending on the starting point is depicted in Figure 8.

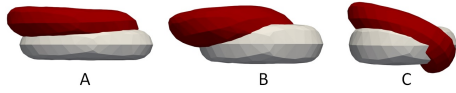


Figure 7: Deformation of cells with different starting positions.

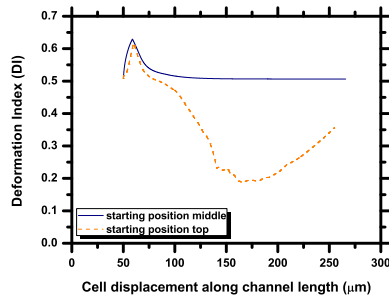


Figure 8: DI of cells with different starting positions.

At the moment limited information could be obtained from the simulations. To save time, the cells with $10\ \mu\text{m}$ in size were positioned before the constriction. We can compare the DI at the beginning of the constriction (at position $66\ \mu\text{m}$ from the beginning of the channel). The average DI of biological cells is 0.65, while for the cell from the simulation, it is 0.58. The difference can be explained by the fact that the DI from simulation comes from one cell position at a certain place and the experimental value is obtained as an average of several cells.

3.4 Channels for Observing CFL

The cell-free layer (CFL) is a hemodynamic phenomenon that contributes to the rheological properties of blood flowing in microvessels. Due to the high shear stresses developed around the wall and the parabolic velocity profile, deformable RBCs in narrower vessels tend to migrate toward the centre of the vessel. This results in the formation of two phases, the central cell concentrated phase and the cell-free liquid phase. To the contrary, white blood cells and platelets that are more rigid than RBCs, as well as more infected RBCs, are localized closer to CFL.

Several factors, such as cell deformability, hematocrit, blood flow rate and vascular geometry, affect the thickness of the resulting CFL. The computational study performed in (Smiešková and Bachratá, 2019), simulated blood flow in a straight channel with different hematocrit values ranging from 5 to 15% with

cells of different stiffness. When examining the impact of the geometry, it is possible to use the microchannels with narrower parts. Section 3.4.1 discusses several challenges we encountered with these in-silico experiments.

New microfluidic chips are now being produced at Metrics in the University of Minho, with different geometries. Our goal is to gather data from these devices at different levels of flow and hematocrits and access more detailed information in order to improve our model for these types of more dense flows. For now, we obtained data from channel design shown in Figure 9.

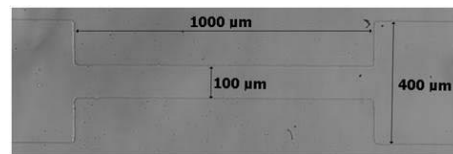


Figure 9: Dimensions of channels for observing CFL. The height of the channel is $30\ \mu\text{m}$.

3.4.1 Simulating Dense Blood Suspensions - Challenges

Simulations of real biological experiments require the use of large-scale computations. It is necessary to choose the degree of simulation complexity based on biological phenomena. One way to simplify the model is to reduce the discretization of the cell membrane. This has a more pronounced effect at higher hematocrits.

The advantage of PyOIF is the possibility to simulate periodic properties of the flow in all three directions. Application of periodic boundary conditions is advantageous for microchannels with a periodic obstacle field (Bušík et al., 2016) or direct microchannels without obstacles (Qi and Shaqfeh, 2017; Smiešková and Bachratá, 2019).

A different situation occurs in the case of channels with complex segmented geometry. In (Pinho et al., 2013), a continuous microfluidic device for partial red blood cell (RBC) extraction and subsequent measurement of RBC deformability was presented. First part of this device, a constriction with different heights (25%, 50% and 75% of the channel height) was placed and the effect of the constriction on the CFL thickness and the effectiveness of the subsequent separation were examined.

Simulating this part of the microfluidic device with the original dimensions ($2500 \times 100 \times 51 / 300 \times 25(50, 75) \times 51 / 100 \times 100 \times 51$) and with a hematocrit of about 9% would represent a seeding of 12900 to 13700 cells. A possible solution to this type of

problem is to divide the entire simulated channel into two consecutive simulations. The first simulation box would have a cuboid shape and would represent a straight part of the channel before the constriction. When the steady-state CFL thickness is reached, the actual cell positions and forces acting on all computational nodes would be stored. This data would be an input to the second simulation box containing the constriction, providing an approximation of the hydrodynamic properties. The open question remains, i.e. the effect of such an approximation on the results, as well as the reduction of computational power or efficiency of such an approach.

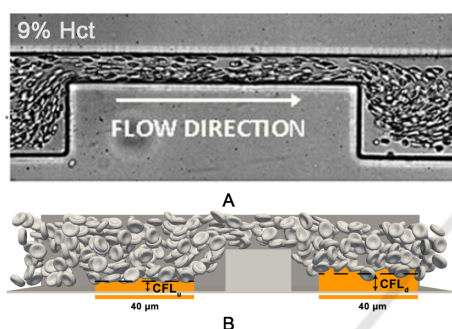


Figure 10: Comparison of the screenshot (A) from a biological experiment (Pinho et al., 2013) and (B) a computational model to investigate the effect of CFL enhancement after insertion of the contraction region into a direct microchannel.

4 CONCLUSIONS

The work presented here addresses a strategy combining an experimental and a numerical approach to develop microfluidic devices focusing diagnostics based on cell deformation and fluid flow behaviour. Microfluidic devices can get blocked with either cells, micro-particles or even some material from the microfluidic channel itself. Saving the data from recorded video takes time, and it is not certain to obtain the desired data at proper conditions. Experimental data is therefore of paramount importance to devise and validate a numerical model, but all the aforementioned issues limit the number of experiments that can be performed. Here is where computational tools can provide help. Before even starting an experiment there is a possibility to run several experimental set up scenarios and based on the analyses of those, it is easier to establish the plan of experiments to perform. An important part of the development of the computational model is the calibration and verification of its functionality. This process is required for different types of cells used in the biological experiments, such

as cell RBC, various types of CTC and many others. For these purposes more simple designs of microfluidic channels can be used as proposed in our paper. It is important to know all the essential parameters of a given biological experiment. When conducting fluid flow simulations, it is essential to know the flow information (Slavík et al., 2017), fluid density and viscosity, channel shape and size.

This work presents several types of microfluidic devices and gives a brief overview of most of the steps necessary to gather data from biological experiments and how to set up simulations using the open-source software Espresso with extension PyOIF. The main focus is towards the development of new microfluidic devices allowing the study of cell deformation and deepen the knowledge on this topic, for future use in alternative diagnostics. Partial results of a simulation are shown and compared with experimental data obtained for the channels with narrow constriction. This procedure shows the usefulness of the calibrated RBC model for healthy RBC. Finally, we outline the possible applications of the simulation tool for optimizing designs of some of these devices.

ACKNOWLEDGEMENTS

This work was supported by the Slovak Research and Development Agency (contract number APVV-15-0751) and by the Ministry of Education, Science, Research and Sport of the Slovak Republic (contract No. VEGA 1/0643/17). Authors are also grateful to Fundação para a Ciência e Tecnologia (FCT) for partially financing the research under the framework of project UTAP-EXPL/CTE/0064/2017 and project n° 030171 financed by LISBOA-01-0145-FEDER-030171 / PTDC/EME-SIS/30171/2017 which also provided a fellowship. Finally authors also grateful to FCT for the IF 2015 recruitment program (IF 00810-2015) and exploratory project associated with this contract.

REFERENCES

- Bachratý, H., Kovalčíková, K., Bachratá, K., and Slavík, M. (2017). Methods of exploring the red blood cells rotation during the simulations in devices with periodic topology. In *2017 International Conference on Information and Digital Technologies (IDT)*, pages 36–46. IEEE.
- Boas, L., Faustino, V., Lima, R., Miranda, J., Minas, G., Fernandes, C., and Catarino, S. (2018). Assessment of the deformability and velocity of healthy and artificially impaired red blood cells in narrow poly-

- dimethylsiloxane (pdms) microchannels. *Micromachines*, 9(8):384.
- Bušík, M. and Cimrák, I. (2017). The calibration of fluid-object interaction in immersed boundary method. In *EPJ Web of Conferences*, volume 143, page 02013. EDP Sciences.
- Bušík, M., Jančígová, I., Tóthová, R., and Cimrák, I. (2016). Simulation study of rare cell trajectories and capture rate in periodic obstacle arrays. *Journal of Computational Science*, 17:370–376.
- Chen, J., Li, J., and Sun, Y. (2012). Microfluidic approaches for cancer cell detection, characterization, and separation. *Lab on a Chip*, 12(10):1753–1767.
- Chovanec, M., Bachratý, H., Jasenčáková, K., and Bachratá, K. (2019). Convolutional neural networks for red blood cell trajectory prediction in simulation of blood flow. In *International Work-Conference on Bioinformatics and Biomedical Engineering*, pages 284–296. Springer.
- Cimrák, I., Gusenbauer, M., and Jančígová, I. (2014). An espresso implementation of elastic objects immersed in a fluid. *Computer Physics Communications*, 185(3):900–907.
- Cimrák, I. and Jančígová, I. (2018). *Computational Blood Cell Mechanics: Road Towards Models and Biomedical Applications*. CRC Press.
- Dao, M., Lim, C. T., and Suresh, S. (2003). Mechanics of the human red blood cell deformed by optical tweezers. *Journal of the Mechanics and Physics of Solids*, 51(11-12):2259–2280.
- Gleghorn, J. P., Pratt, E. D., Denning, D., Liu, H., Bander, N. H., Tagawa, S. T., Nanus, D. M., Giannakakou, P. A., and Kirby, B. J. (2010). Capture of circulating tumor cells from whole blood of prostate cancer patients using geometrically enhanced differential immunocapture (gedi) and a prostate-specific antibody. *Lab on a chip*, 10(1):27–29.
- Hou, H. W., Li, Q., Lee, G., Kumar, A., Ong, C., and Lim, C. T. (2009). Deformability study of breast cancer cells using microfluidics. *Biomedical microdevices*, 11(3):557–564.
- Huang, L. R., Cox, E. C., Austin, R. H., and Sturm, J. C. (2004). Continuous particle separation through deterministic lateral displacement. *Science*, 304(5673):987–990.
- Inglis, D. W., Davis, J. A., Austin, R. H., and Sturm, J. C. (2006). Critical particle size for fractionation by deterministic lateral displacement. *Lab on a Chip*, 6(5):655–658.
- Kajánek, F. and Cimrák, I. (2019). Evaluation of detection of red blood cells using convolutional neural networks. In *2019 International Conference on Information and Digital Technologies (IDT)*, pages 198–202. IEEE.
- Kovalčíková, K. (2019). Discretization of simulation elements—feasibility limits and accuracy of results. In *2019 Proceedings of MIST Conference on Mathematics in Science and Technologies (2019, In press)*.
- Kovalčíková, K., Slavík, M., Bachratá, K., Bachratý, H., and Bohiniková, A. (2018). Volumetric flow rate in simulations of microfluidic devices. In *EPJ Web of Conferences*, volume 180, page 02046. EDP Sciences.
- Lima, R., Ishikawa, T., Imai, Y., Takeda, M., Wada, S., and Yamaguchi, T. (2008). Radial dispersion of red blood cells in blood flowing through glass capillaries: the role of hematocrit and geometry. *Journal of biomechanics*, 41(10):2188–2196.
- Nagrath, S., Sequist, L. V., Maheswaran, S., Bell, D. W., Irimia, D., Utkus, L., Smith, M. R., Kwak, E. L., Digumarthy, S., Muzikansky, A., et al. (2007). Isolation of rare circulating tumour cells in cancer patients by microchip technology. *Nature*, 450(7173):1235.
- Pinho, D., Yaginuma, T., and Lima, R. (2013). A microfluidic device for partial cell separation and deformability assessment. *BioChip Journal*, 7(4):367–374.
- Qi, Q. M. and Shaqfeh, E. S. (2017). Theory to predict particle migration and margination in the pressure-driven channel flow of blood. *Physical Review Fluids*, 2(9):093102.
- Sajeesh, P. and Sen, A. K. (2014). Particle separation and sorting in microfluidic devices: a review. *Microfluidics and nanofluidics*, 17(1):1–52.
- Schneider, C. A., Rasband, W. S., and Eliceiri, K. W. (2012). Nih image to imagej: 25 years of image analysis. *Nature methods*, 9(7):671.
- Shields IV, C. W., Reyes, C. D., and López, G. P. (2015). Microfluidic cell sorting: a review of the advances in the separation of cells from debulking to rare cell isolation. *Lab on a Chip*, 15(5):1230–1249.
- Slavík, M., Bachratá, K., Bachratý, H., and Kovalčíková, K. (2017). The sensitivity of the statistical characteristics to the selected parameters of the simulation model in the red blood cell flow simulations. In *2017 International Conference on Information and Digital Technologies (IDT)*, pages 344–349. IEEE.
- Smiešková, M. and Bachratá, K. (2019). Validation of bulk properties of red blood cells in simulations. In *2019 International Conference on Information and Digital Technologies (IDT)*, pages 417–423. IEEE.
- Warkiani, M. E., Guan, G., Luan, K. B., Lee, W. C., Bhagat, A. A. S., Chaudhuri, P. K., Tan, D. S.-W., Lim, W. T., Lee, S. C., Chen, P. C., et al. (2014). Slanted spiral microfluidics for the ultra-fast, label-free isolation of circulating tumor cells. *Lab on a Chip*, 14(1):128–137.
- Weik, F., Weeber, R., Szuttor, K., Breitsprecher, K., de Graaf, J., Kuron, M., Landsgesell, J., Menke, H., Sean, D., and Holm, C. (2019). Espresso 4.0 – an extensible software package for simulating soft matter systems. *The European Physical Journal Special Topics*, 227(14):1789–1816.
- Zhang, Z. and Nagrath, S. (2013). Microfluidics and cancer: are we there yet? *Biomedical microdevices*, 15(4):595–609.